Ductility of Non-Compact Steel Bridge Beams

SAMI W. TABSH, Ph.D., P.E.

INTRODUCTION

Since the fifties, composite construction in steel bridges has been used in simple as well as in continuous structures. Composite construction incorporates the concrete deck with the top flange of the supporting rolled beams or welded plate girders. The final result consists of the two components from different materials acting as a unit. The composite action can be accomplished by mechanical bond between the flange and deck in the form of welded channels, studs, or other devices. Either shored or unshored construction can be specified.

Composite construction for highway bridge design is most economical for spans in the range of 40–50 ft. and longer. The increase in the moment of inertia of the composite section helps in reducing deflection due to live load and impact. For shorter spans, the saving in steel weight does not usually pay for the additional weight of the shear connections and labor involved.

Composite steel girder bridges in the United States are usually designed using the Load Factor Design procedure of AASHTO's Standard Specifications for Highway Bridges.[1] Current AASHTO allows the bending moment capacity of compact sections in positive bending to be based on the full plastic moment. The moment capacity at first yield is used, however, for non-compact sections. In most practical cases, the full plastic moment of composite sections is significantly larger than the yield moment.

Compact sections designed by AASHTO need to satisfy requirements related to web and compression-flange slenderness, lateral bracing, and ductility. Experience has shown that in most cases, composite sections under the maximum design loads easily satisfy the web slenderness requirement because often the majority of the web is in tension. Further, the compression-flange and lateral bracing requirements do not apply for this type of construction under the maximum design loads since the top steel flange is adequately braced by the hardened concrete deck. However, the limitations on the compression flange slenderness and lateral bracing must be checked for dead load on the non-composite section during construction. Therefore, the only other criterion that needs to be satisfied under the maximum design loads is the ductility requirement.

Sami W. Tabsh, Ph.D., P.E., is project engineer, Gannett Fleming, Inc., Harrisburg, PA.

The purpose of AASHTO's ductility requirement, as specified in Equation 10-128a of the Specifications, is to ensure that the strain in the tension flange of the steel section is significantly above the yield strain before the onset of concrete crushing at the top of the deck. This requirement limits the total compression depth of the composite section from the top of the concrete deck to the plastic neutral axis to a maximum of 13.3 percent of the total depth of the composite section. For a W36 section with an 8-in. concrete slab, the plastic neutral axis has to be less than 5.9 in. from the top of the slab in order for this section to be classified as compact. Thus, such sections rarely qualify as compact according to the current criterion. Further, some rolled beams have cover plates welded to the outer face of the bottom flange, thus shifting the plastic neutral axis further downward.

The objective of this study is to investigate the ductility of simply supported composite rolled beams that satisfy all compactness requirements except the one pertaining to ductility. Typical sections in positive bending are analyzed for a profile of curvature. A parametric study is carried out to investigate the effect of variation in some design variables on ductility. These design variables include the grade of structural steel, concrete strength, deck dimensions and reinforcement, depth of steel beam, and presence of a cover plate.

DUCTILITY MEASURE

Moment-curvature (M–ϕ) relationships can be used to investigate the ductility of sections in flexure. The shape of the M–ϕ curve depends on the section dimensions, material strength and distribution, and the presence of axial loads. Curvature, by definition, is the rotation per unit length. Therefore, the rotation, θ, between points A and B on the member shown in Figure 1 can be obtained from curvature, ϕ, as follows:

$$\theta_{AB} = \int_A^B \phi dx \qquad (1)$$

where dx is an element along the length of the member. For elastic behavior, curvature can be obtained from the bending moment and flexural stiffness

$$\phi = \frac{M}{EI} \qquad (2)$$

where M is the bending moment, E is Young's modulus, and I is the moment of inertia. It should be noted that Equation 2 does not hold for inelastic behavior.[2]

The deflection of point A in Figure 1 from the tangent of the member at point B can be evaluated from the following integral:

$$\Delta_{AB} = \int_A^B x\phi dx \tag{3}$$

Equations 1 and 3 are generalizations of the moment-area theorems, and they apply whether elastic or plastic curvatures are involved.

There are many approaches for measuring ductility of members in flexure. In general, ductility measures are usually derived based on the ratio of the maximum deformation to the deformation at the onset of yielding. Ductility can be assessed in terms of curvature, ϕ, deflection, Δ, or rotation, θ, as follows:

$$\eta_{cur} = \frac{\phi_{max}}{\phi_y} \tag{4}$$

$$\eta_{def} = \frac{\Delta_{max}}{\Delta_y} \tag{5}$$

$$\eta_{rot} = \frac{\theta_{max}}{\theta_y} \tag{6}$$

where η_{cur}, η_{def}, and η_{rot} are curvature, deflection, and rotation ductility ratios, respectively. The maximum curvature, deflection, and rotation (ϕ_{max}, Δ_{max}, and θ_{max}) and are normally obtained at the point at which the concrete reaches a maximum strain in compression equal to 0.003, even though the section can sustain the applied moment with additional deformation (ductility) at a concrete strain level beyond 0.003. The use of η_{cur} as a measure of ductility has an advantage because it is a function of the cross-sectional geometric and strength properties only. η_{def} and η_{rot}, on the other hand, require additional information related to the span length, support conditions, and loading configuration.

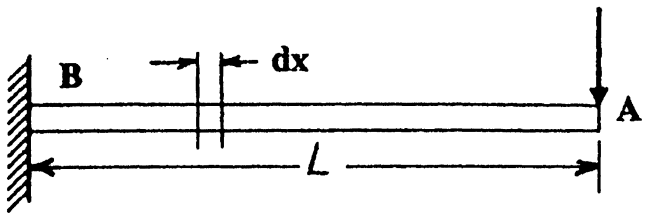

Fig. 1. Cantilever beam.

MOMENT-CURVATURE RELATIONSHIP

Complete generation of the M–ϕ curve for a composite section is a time-consuming process. The reason for this is because detailed stress-strain relationships in compression as well as in tension of all materials in the cross section are needed. The strain incremental approach[3] is used in this study to generate the M–ϕ relationship. This method is particularly useful to implement in composite sections. The analysis starts by idealizing the section by a set of uniform layers, as shown in Figure 2. Next, a strain diagram is assumed and the corresponding stress diagram is generated using the non-linear stress-strain relationships for the materials. The total compressive force for the layers above the neutral axis is obtained by multiplying the average stress at a layer by the area and summing up the forces for all layers. The total force in tension below the neutral axis can also be obtained in a similar fashion. For the assumed strain diagram, the total compressive force should be equal to the tensile force, or else there is no equilibrium across the section. The strain diagram can be modified based on the difference between compressive and tensile stresses. The moment and curvature corresponding to the correct strain diagram are then evaluated. Strain at the top is increased gradually by increments and the procedure is continued until a specified ultimate strain at the top of the concrete slab is attained.

Figure 3 shows a typical M–ϕ curve for a composite steel beam. The section is composed of a 72-in. wide by 8-in. thick concrete slab and a W36×230 beam, separated by a 1-in. thick concrete haunch above the top flange. Top reinforcement in the slab is composed of No. 4 bars at 12 in., whereas bottom reinforcement is No. 5 bars at 12 in. A specified 28-day concrete compressive strength of 4,000 psi is specified for the deck, Grade 60 steel for the rebars, and AASHTO M270 Grade 36 structural steel for the rolled beam. The calculations are carried out until the strain at the top of the slab, ε_c, attains a maximum value of 0.005. The results of the analysis indicate that the value of η_{cur} is equal to 6.84 when $\varepsilon_c = 0.003$, 8.81 when $\varepsilon_c = 0.004$, and 10.42 when $\varepsilon_c = 0.005$. The moment capacity at $\varepsilon_c = 0.005$ is about 5.5 percent smaller than the moment capacity at $\varepsilon_c = 0.003$.

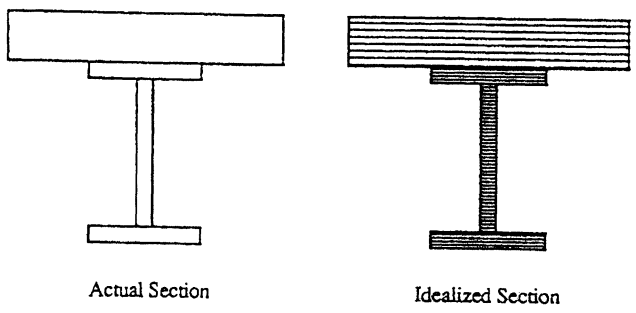

Fig. 2. Strain incremental approach.

MATERIAL MODELING

As stated earlier, material stress-strain relationships are needed for the development of moment-curvature relationships using the strain incremental approach. In this study, the relationship between stress, f_c, and strain, ε_c, for concrete under compression is modeled by a Hognestad parabola with a linear tail[4], as shown in Figure 4. The parabola is expressed by

$$f_c = f_c'\left[2\left(\frac{\varepsilon_c}{\varepsilon_o}\right) - \left(\frac{\varepsilon_c}{\varepsilon_o}\right)^2\right] \tag{7}$$

and the tail is expressed by the following straight-line relationship:

$$f_c = f_c'[1 - Z(\varepsilon_c - \varepsilon_o)] \tag{8}$$

where

f_c' = the 28-day concrete compressive strength

ε_o = concrete strain at f_c', taken equal to 0.002

Z is a constant related to the slope of the straight line. For unconfined concrete, Z can be evaluated from the following expression:

$$Z = \frac{0.5}{\varepsilon_{50} - \varepsilon_o} \tag{9}$$

where ε_{50} is the concrete strain beyond ε_o at which the concrete stress on the stress-strain curve drops to $0.5f_c'$. ε_{50} is a function of f_c' only as follows:

$$\varepsilon_{50} = \frac{3 + 0.002f_c'}{f_c' - 1{,}000} \tag{10}$$

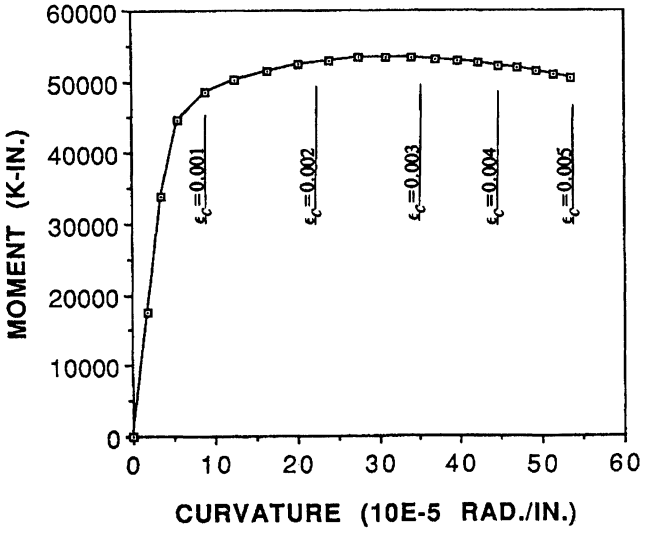

Fig. 3. M–ϕ curve for a W36×230 *composite beam.*

where f_c' is in psi.

The stress-strain curve for concrete in tension is approximated by a linear relationship. The maximum stress at rupture, f_r, is equal to

$$f_r = 7.5\sqrt{f_c'} \tag{11}$$

where both f_r and f_c' are in psi.

Material behavior for steel in tension is shown in Figure 5. If residual stresses are ignored, then the relationship between the steel stress, F_s, and the strain, ε_s, can be modeled by three segments,

1. For $\varepsilon_s \le \varepsilon_y$:

$$F_s = E_s \varepsilon_s \tag{12}$$

2. For $\varepsilon_y < \varepsilon_s \le \varepsilon_h$:

$$F_s = F_y \tag{13}$$

3. For $\varepsilon_h < \varepsilon_s \le \varepsilon_u$:

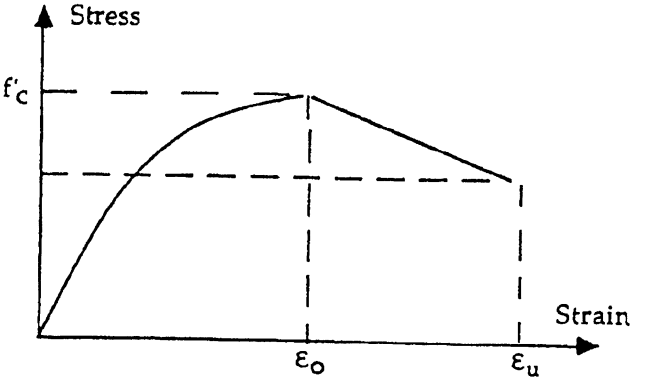

Fig. 4. Stress-strain curve for concrete.

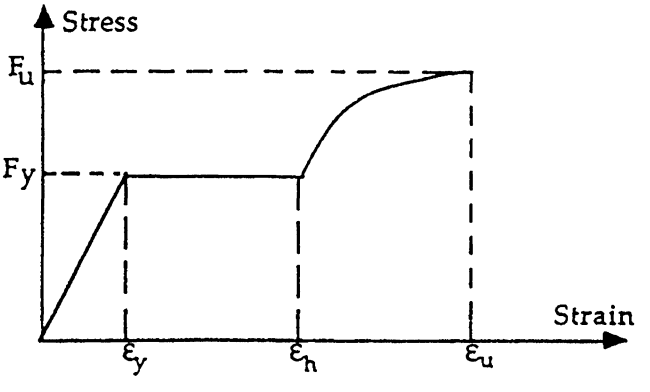

Fig. 5. Stress-strain curve for steel.

Table 1. Critical Points on the Stress-Strain Curve for Steel						
Steel Type	Grade	ε_y	ε_h	ε_u	F_y	F_u
Reinforcing	60	0.0021	0.008	0.10	60 ksi	108 ksi
Structural	36	0.0012	0.014	0.20	36 ksi	58 ksi
	50	0.0017	0.021	0.19	50 ksi	65 ksi

$$F_s = F_y + (F_u - F_y)\left[2\left(\frac{\varepsilon_s - \varepsilon_h}{\varepsilon_u - \varepsilon_h}\right) - \left(\frac{\varepsilon_s - \varepsilon_h}{\varepsilon_u - \varepsilon_h}\right)^2\right] \quad (14)$$

where ε_y, ε_h, and ε_u are steel strains at yield, initiation of strain hardening, and at the ultimate tensile stress, respectively. Also, F_y and F_u are respectively the yield stress and the ultimate tensile stress. The modulus of elasticity of steel in the elastic range, E_s, may be taken equal to 29,000 ksi.

The expressions in Equations 12 through 14 can be used to model the behavior of reinforcing steel as well as structural steel. The only difference is in the selection of the appropriate values for the stress and strain at yield, strain hardening, and ultimate. Typical values[5,6] at the critical points for Grade 60 reinforcing steel and AASHTO M270 Grades 36 and 50 structural steels are presented in Table 1.

REINFORCED CONCRETE VERSUS COMPOSITE STEEL

Structural design specifications usually impose certain limitations on the design variables in order to have reasonable assurance of a ductile failure mode in flexure. For example, AASHTO limits the steel reinforcement ratio, ρ, in reinforced concrete beams to a maximum value equal to

$$\rho \le 0.75\rho_b \quad (15)$$

where ρ_b is the balanced reinforcement ratio. Balanced conditions occur when the maximum concrete strain in compression reaches a value of 0.003 at the time the tension steel starts to yield.

In a similar fashion, and to ensure adequate ductility in composite steel beams and girders, AASHTO requires the distance from the top of the slab to the neutral axis in plastic bending, D_p, of compact sections in positive bending not to exceed the following value:

$$D_p \le \frac{d + t_s + t_h}{7.5} \quad (16)$$

where d is the depth of steel section, t_s is the thickness of concrete slab, and t_h is the thickness of the concrete haunch above the top flange.

The ductility of typical reinforced concrete T-beams is compared with the ductility of composite steel beams. Two different size cross sections of T-beams with various steel depths are considered in the analysis. One cross section is composed of a 72-in. wide by 6-in. thick flange with an 18-in. wide web, whereas the second is composed of a 108-in. wide by 7-in. thick flange with a 24-in. wide web, as shown in Figure 6. The steel reinforcement depth from the top of the section varied between 24 in. and 60 in. Further, two levels of steel reinforcement are investigated for the T-beams: 75 percent and 62.5 percent of the balanced reinforcement ratio. In all cases, the center of gravity of the tension reinforcement is assumed to be 6 in. from the bottom of the beam. Concrete 28-day compressive strength of 4,000 psi and Grade 60 steel for the rebars are specified. Compression steel in the flange is ignored due to its minor effect on the strength and ductility.

The complete findings of the ductility analysis for the considered T-beams are summarized in Tables 2 and 3. Typical M–ϕ curves for T-beams with a 72-in. by 6-in. flange and 18-in. web having $\rho = 0.75\rho_b$ are shown in Figure 7. The results showed that η_{cur} for the case of $\rho = 0.75\rho_b$ varied between 2.77 and 3.50, with an average value of 3.13. The corresponding range of η_{cur} for the case of $\rho = 0.625\rho_b$ is 3.96 to 5.33, with an average value equal to 4.82.

The flexural behavior of non-compact composite steel beams is investigated by considering 32 different cross sections. The cross sections are composed of either a 72-in. by 8-in. or a 108-in. by 9-in. concrete slab, 1-in. thick concrete

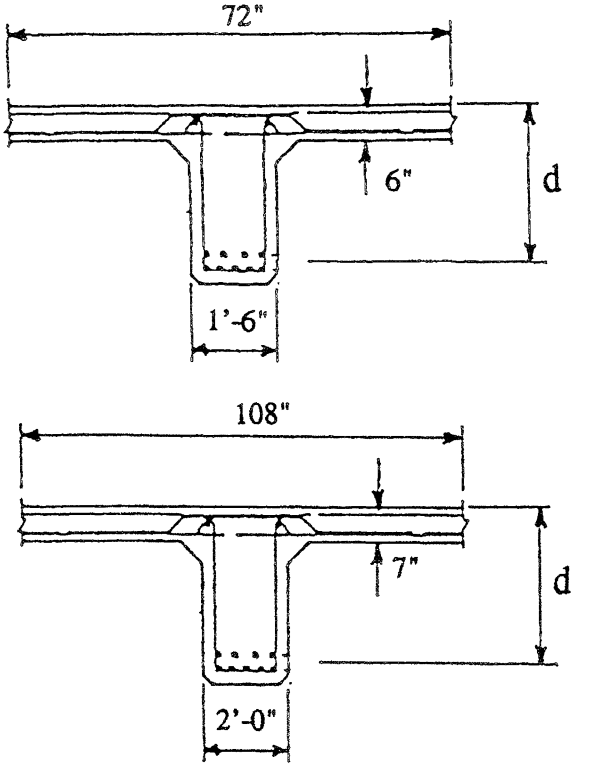

Fig. 6. Reinforced concrete T-beams considered in the study.

Table 2.
η_{cur} for Reinforced Concrete T-Sections with $\rho = 0.75\rho_b$

Section Number	b (in.)	t_s (in.)	d (in.)	ϕ_y (10^{-5} Rad/in.)	ϕ_{max} (10^{-5} Rad/in.)	η_{cur}
1	72.0	6.0	24.0	14.8	44.8	3.03
2	72.0	6.0	36.0	9.80	31.7	3.24
3	72.0	6.0	48.0	7.43	20.6	2.77
4	108.0	7.0	36.0	9.76	34.2	3.50
5	108.0	7.0	48.0	7.34	24.5	3.34
6	108.0	7.0	60.0	5.89	16.9	2.87

Table 3.
η_{cur} for Reinforced Concrete T-Sections with $\rho = 0.625\rho_b$

Section Number	b (in.)	t_s (in.)	d (in.)	ϕ_y (10^{-5} Rad/in.)	ϕ_{max} (10^{-5} Rad/in.)	η_{cur}
7	72.0	6.0	24.0	13.9	55.2	3.96
8	72.0	6.0	36.0	9.14	44.3	4.85
9	72.0	6.0	48.0	6.95	33.4	4.80
10	108.0	7.0	36.0	9.00	43.1	4.79
11	108.0	7.0	48.0	6.77	36.1	5.33
12	108.0	7.0	60.0	5.48	28.5	5.20

haunch, and a rolled steel beam, as shown in Figure 8. The wide-flange steel sections vary in size between W33×130 and W36×300. A concrete compressive strength of 4,000 psi is specified for the slab and AASHTO M270 Grades 36 or 50 structural steels are specified for the rolled beams. For simplicity, the reinforcement in the concrete deck is neglected in the analysis. Investigation of the above composite steel beams in plastic bending indicated that all but three do not satisfy the above ductility requirement of Equation 16. Therefore, 29 out of the 32 considered cross sections are non-compact according to the AASHTO Specifications.

Tables 4 and 5 present the complete results of the ductility analysis for AASHTO M270 Grades 36 and 50 steels, respectively. The analysis of the non-compact sections with Grade 36 steel showed that η_{cur} varies between 6.74 and 11.4, with an average value of 9.27. The range of η_{cur} for Grade 50 steel is 3.80 to 9.61, and the average is 6.19. In general, composite beams made with Grade 50 steel had 40 percent less ductility than composite beams made with Grade 36 steel. The relationship between η_{cur} and the ratio of D_p-to-$(d + t_s + t_h)/7.5$ is investigated in Figure 9. A ratio of D_p-to-$(d + t_s + t_h)/7.5$ smaller than 1.0 indicates a non-compact section according to the Specifications. Figure 9 shows that an increase in the ratio of D_p-to-$(d + t_s + t_h)/7.5$, as suggested by AASHTO, accurately predicts a decrease in η_{cur}. However, the relationship between the two variables is highly non-linear and is not the same for the two grades of steel considered. The ratio of D_p-to-$(d + t_s + t_h)/7.5$ appears to penalize composite beams with Grade 36 steel much more than composite beams with Grade 50 steel. Typical generated M–ϕ curves for Grade 36 composite steel beams composed of a 72-in. by 8-in. slab with W33×130, W36×230, and W36×300 rolled sections are shown in Figure 10.

Comparison of the results of the curvature ductility analysis for the considered beams shows that the non-compact composite beams possess more ductility than the reinforced concrete T-beams. On average, the composite beams with Grade 36 steel had about 3 and 2 times the curvature ductility of T-beams with reinforcement ratios equal to $0.75\rho_b$ and $0.625\rho_b$, respectively. The average curvature ductility ratios for composite beams with Grade 50 steel are about 2 and 1.3 times the corresponding ratios for T-beams with reinforcement ratios equal to $0.75\rho_b$ and $0.625\rho_b$, respectively.

PARAMETRIC STUDY

In this section, a parametric study is carried out on a composite steel beam. The purpose of the parametric study is to investigate the sensitivity of the M–ϕ relationship to changes in the steel and concrete strength properties, dimensions of the slab, depth of the steel section, and presence of a bottom flange cover plate. The reference design is composed of a 72-in. wide by 8-in. thick concrete slab, 1-in. thick concrete haunch above the top flange, and a W36×230 steel beam. The 28-day concrete compressive strength in the slab is specified to be 4,000 psi and AASHTO M270 Grade 36 structural steel is specified for the rolled beam. A ductility analysis on the composite beam showed that η_{cur} is equal to 8.16 at $\varepsilon_c = 0.003$. The corresponding nominal moment capacity at this level of strain, M_n, is equal to 4,400 k-ft. The compression depth of the section in plastic bending, D_p, is equal to 9.38 in. This value of D_p does not satisfy the ductility requirement of Equation 16 and thus, the section is non-compact.

The effect of using higher material strengths in the composite beam on the shape of the M–ϕ curve is investigated. Figure 11 shows the results of using AASHTO M270 Grade 50 structural steel in the rolled beam. The results of using 6,000 psi concrete strength in the slab are presented in Figure 12. As expected, the analysis indicates that M_n is more sensitive to changes in steel than in concrete properties. The amount of increase in M_n is equal to 31 percent and 7 percent when using Grade 50 steel and 6,000 psi concrete, respectively. It is interesting, however, to note that η_{cur} decreases by 21 percent with the use of Grade 50 steel, whereas the same quantity increases by 29 percent when 6,000 psi concrete is used.

The effect of a change in the dimensions of the concrete slab is studied in Figures 13 and 14. Figure 13 presents the results of using a thicker slab ($t_s = 12$ in.) and Figure 14 shows the results for a wider deck ($b = 96$ in.). The analysis indicates that a change in t_s affects M_n (18 percent increase) much more than η_{cur} (6 percent decrease). The opposite is true for changes in b (5 percent and 23 percent increase for M_n and η_{cur}, respectively). Figure 15 shows that accounting for No. 8 reinforcing bars at 12 in. at the mid-depth of the concrete slab negligibly affects the flexural capacity at $\varepsilon_c = 0.003$. Also, η_{cur} is slightly increased (up 6 percent) with the rebars present.

Figures 16 and 17 show the results of changes in the geometry of the rolled beam on the shape of the M–ϕ relationship. A 25 percent increase in the depth of the W36×230 increases M_n by 29 percent and η_{cur} by 12 percent, as shown in Figure 16. On the other hand, Figure 17 indicates that welding a 1-in. by 12 in. cover plate to the outer face of the bottom flange results in a 30 percent higher capacity and a 21 percent lower ductility.

SUMMARY AND CONCLUSIONS

The ductility of non-compact composite steel beams in positive bending according to the current AASHTO criteria is studied. Ductility is measured in terms of both a moment-curvature relationship (M–ϕ) and a curvature ductility ratio

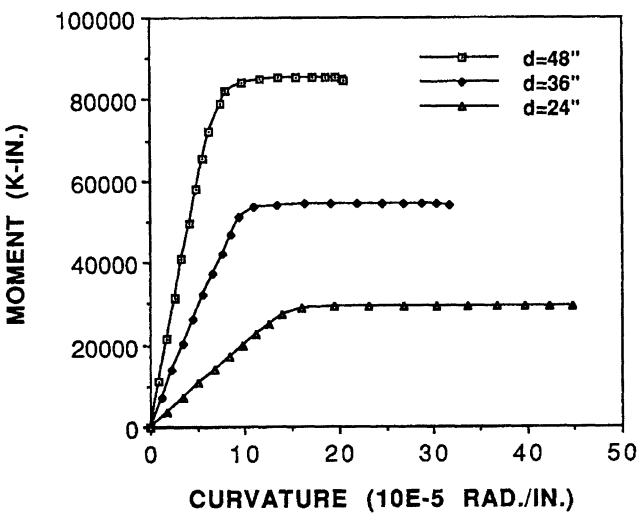

Fig. 7. Composite steel beams considered in the study.

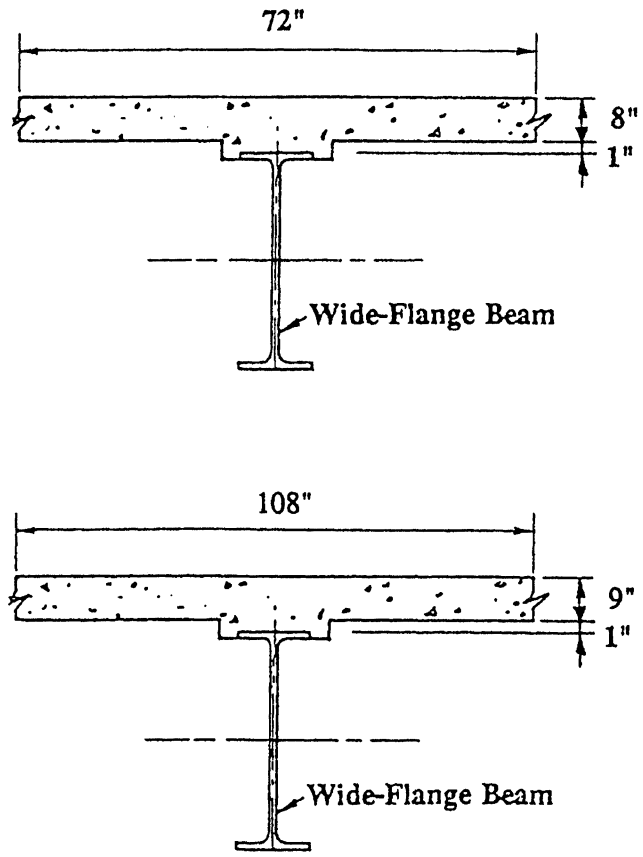

Fig. 8. M–ϕ curves for reinforced concrete T-beams.

PARAMETRIC STUDY

In this section, a parametric study is carried out on a composite steel beam. The purpose of the parametric study is to investigate the sensitivity of the M–ϕ relationship to changes in the steel and concrete strength properties, dimensions of the slab, depth of the steel section, and presence of a bottom flange cover plate. The reference design is composed of a 72-in. wide by 8-in. thick concrete slab, 1-in. thick concrete haunch above the top flange, and a W36×230 steel beam. The 28-day concrete compressive strength in the slab is specified to be 4,000 psi and AASHTO M270 Grade 36 structural steel is specified for the rolled beam. A ductility analysis on the composite beam showed that η_{cur} is equal to 8.16 at $\varepsilon_c = 0.003$. The corresponding nominal moment capacity at this level of strain, M_n, is equal to 4,400 k-ft. The compression depth of the section in plastic bending, D_p, is equal to 9.38 in. This value of D_p does not satisfy the ductility requirement of Equation 16 and thus, the section is non-compact.

The effect of using higher material strengths in the composite beam on the shape of the M–ϕ curve is investigated. Figure 11 shows the results of using AASHTO M270 Grade 50 structural steel in the rolled beam. The results of using 6,000 psi concrete strength in the slab are presented in Figure 12. As expected, the analysis indicates that M_n is more sensitive to changes in steel than in concrete properties. The amount of increase in M_n is equal to 31 percent and 7 percent when using Grade 50 steel and 6,000 psi concrete, respectively. It is interesting, however, to note that η_{cur} decreases by 21 percent with the use of Grade 50 steel, whereas the same quantity increases by 29 percent when 6,000 psi concrete is used.

The effect of a change in the dimensions of the concrete slab is studied in Figures 13 and 14. Figure 13 presents the results of using a thicker slab ($t_s = 12$ in.) and Figure 14 shows the results for a wider deck ($b = 96$ in.). The analysis indicates that a change in t_s affects M_n (18 percent increase) much more than η_{cur} (6 percent decrease). The opposite is true for changes in b (5 percent and 23 percent increase for M_n and η_{cur}, respectively). Figure 15 shows that accounting for No. 8 reinforcing bars at 12 in. at the mid-depth of the concrete slab negligibly affects the flexural capacity at $\varepsilon_c = 0.003$. Also, η_{cur} is slightly increased (up 6 percent) with the rebars present.

Figures 16 and 17 show the results of changes in the geometry of the rolled beam on the shape of the M–ϕ relationship. A 25 percent increase in the depth of the W36×230 increases M_n by 29 percent and η_{cur} by 12 percent, as shown in Figure 16. On the other hand, Figure 17 indicates that welding a 1-in. by 12 in. cover plate to the outer face of the bottom flange results in a 30 percent higher capacity and a 21 percent lower ductility.

SUMMARY AND CONCLUSIONS

The ductility of non-compact composite steel beams in positive bending according to the current AASHTO criteria is studied. Ductility is measured in terms of both a moment-curvature relationship (M–ϕ) and a curvature ductility ratio

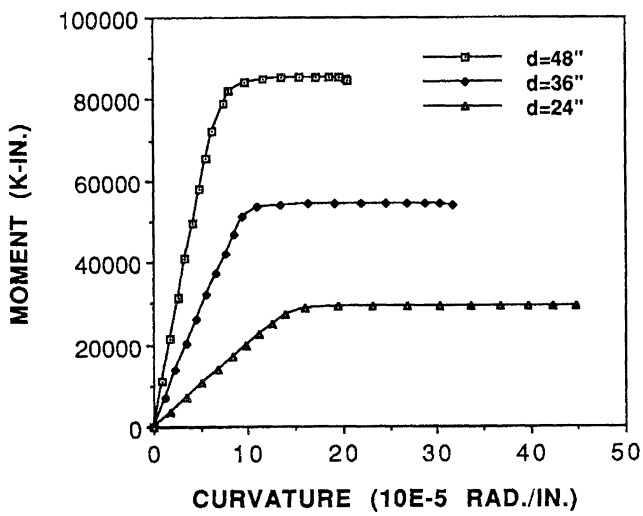

Fig. 7. Composite steel beams considered in the study.

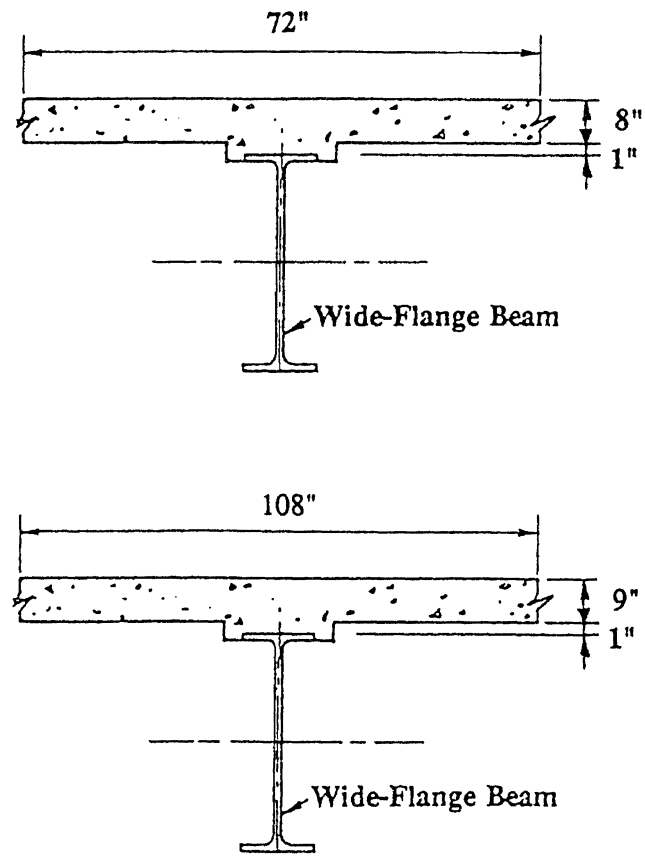

Fig. 8. M–ϕ curves for reinforced concrete T-beams.

Table 4.
η_{cur} for Composite Steel Beams with F_y = 36 ksi

Beam Section	b (in.)	t_s (in.)	$(d + t_s + t_h) / 7.5$ (in.)	D_p (in.)	ϕ_y (10^{-5} Rad/in.)	ϕ_{max} (10^{-5} Rad/in.)	η_{cur}
W36×300	72.0 108.0	8.0 9.0	6.23 6.37	9.99 10.1	4.35 3.85	29.3 34.4	6.74 8.94
W36×280	72.0 108.0	8.0 9.0	6.20 6.34	9.82 9.42	4.29 3.81	30.6 35.7	7.13 9.37
W36×260	72.0 108.0	8.0 9.0	6.17 6.30	9.64 8.73	4.24 3.79	31.9 37.1	7.52 9.79
W36×230	72.0 108.0	8.0 9.0	6.12 6.25	9.38 7.71	4.19 3.76	34.2 39.8	8.16 10.6
W36×210	72.0 108.0	8.0 9.0	6.23 6.36	9.28 7.07	4.05 3.64	35.0 42.7	8.64 11.7
W36×182	72.0 108.0	8.0 9.0	6.18 6.31	9.19 6.13	3.94 3.57	37.9 49.2	9.62 13.8*
W36×150	72.0 108.0	8.0 9.0	6.11 6.25	7.57 5.05	3.86 3.50	42.1 59.7	10.9 17.1*
W33×130	72.0 108.0	8.0 9.0	5.75 5.88	6.55 4.37	4.07 3.70	46.1 69.0	11.4 18.6*

* These sections are compact.

Table 5.
η_{cur} for Composite Steel Beams with F_y = 50 ksi

Beam Section	b (in.)	t_s (in.)	$(d + t_s + t_h) / 7.5$ (in.)	D_p (in.)	ϕ_y (10^{-5} Rad/in.)	ϕ_{max} (10^{-5} Rad/in.)	η_{cur}
W36×300	72.0 108.0	8.0 9.0	6.23 6.37	10.5 10.6	6.16 5.42	23.4 29.9	3.80 5.52
W36×280	72.0 108.0	8.0 9.0	6.20 6.34	10.3 10.5	6.07 5.40	24.6 31.2	4.05 5.78
W36×260	72.0 108.0	8.0 9.0	6.17 6.30	10.1 10.3	5.99 5.33	26.0 32.5	4.34 6.10
W36×230	72.0 108.0	8.0 9.0	6.12 6.25	9.84 10.0	5.91 5.24	28.4 34.8	4.81 6.64
W36×210	72.0 108.0	8.0 9.0	6.23 6.36	9.91 9.82	5.66 5.08	28.7 35.9	5.07 7.07
W36×182	72.0 108.0	8.0 9.0	6.18 6.31	9.58 8.51	5.56 5.00	31.9 39.1	5.74 7.82
W36×150	72.0 108.0	8.0 9.0	6.11 6.25	9.19 7.01	5.39 4.90	36.2 43.9	6.72 8.96
W33×130	72.0 108.0	8.0 9.0	5.75 5.88	9.10 6.07	5.66 5.17	39.5 49.7	6.98 9.61

(η_{cur}). The analytical strain incremental procedure is used to generate complete M–ϕ curves of typical sections using material stress-strain models. A parametric study is carried out in order to find the sensitivity of the M–ϕ relationship and η_{cur} to changes in strength and geometric variables. The results of this study lead to the following conclusions:

1. η_{cur} represents a rational and simple method for measuring ductility in bridge girders under flexural loading.
2. The non-compact composite steel beams with Grades 36 and 50 steels analyzed in this study possessed more ductility than the considered reinforced concrete T-beams, which were designed to satisfy either 75 percent or 62.5 percent of the balanced reinforcement ratio.
3. The ductility requirement, as expressed in terms of Equation 10-128a of the AASHTO Specifications, appears to be very conservative, especially when the grade of steel is low.
4. Ductility is most sensitive to changes in material strengths, concrete slab width, and the presence of a cover plate.
5. Ultimate moment capacity is mostly affected by changes in grade of the structural steel, thickness of the concrete deck, depth of steel beam, and dimensions of cover plate.
6. Ductility increases with an increase in concrete compressive strength, width of deck, depth of steel beam, and reinforcement of deck. It decreases with an increase

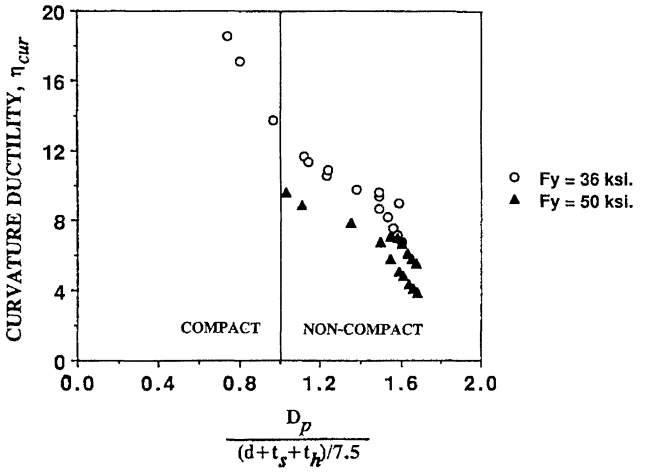

Fig. 9. M–ϕ curves for composite steel beams.

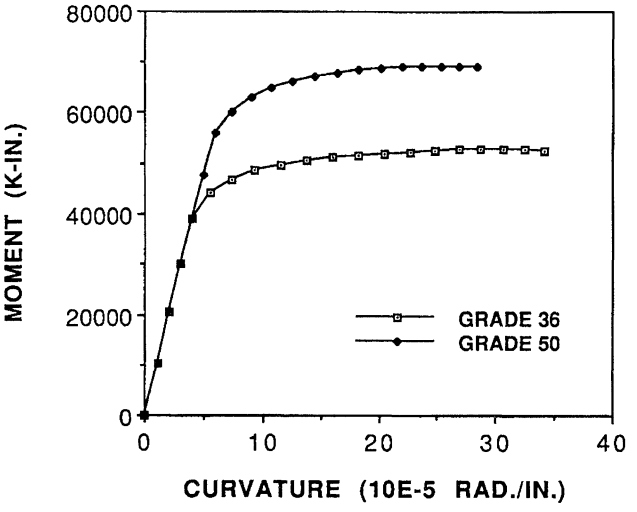

Fig. 11. Effect of steel grade on M–ϕ curve.

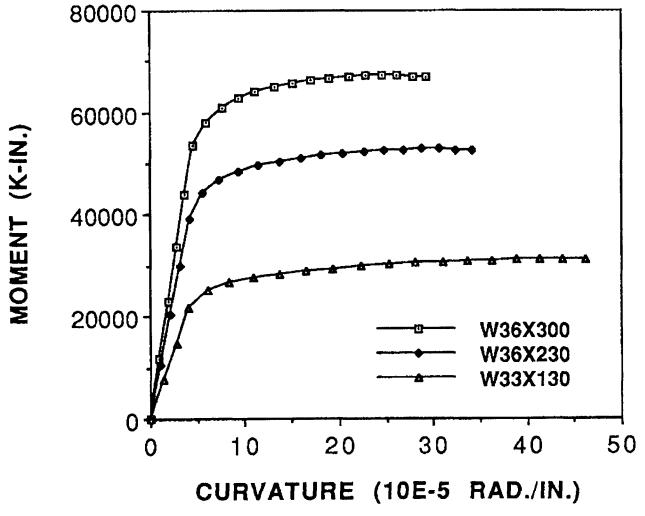

Fig. 10. η_{cur} for composite steel beams.

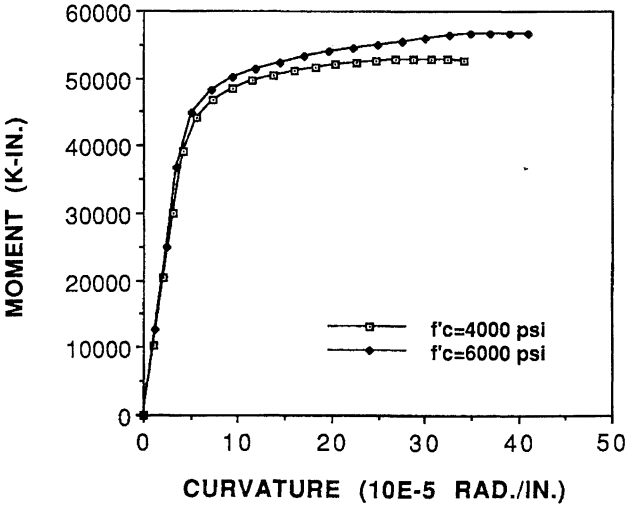

Fig. 12. Effect of f_c' on M–ϕ curve.

in the grade of the structural steel and with the presence of a cover plate.

It should be mentioned that additional analytical and experimental studies on the ductility of composite steel beams are needed to support the above findings. It is expected that further research will lead to specification revisions in the near future.

ACKNOWLEDGMENTS

The author would like to thank Gannett Fleming, Inc., for allowing him to use the computer facilities. The encouragement of Mr. Ronald Drnevich, Senior Vice President and Head of Transportation Division, and Mr. Russ Ricker, Manager of Bridge Section, is very much appreciated. Special thanks are due to Mr. David Marchese for developing a spread-sheet program for AASHTO design and to Mrs. Sanaa Khalifeh for generating the illustrations.

REFERENCES

1. American Association of State Highway and Transportation Officials, *Standard Specifications for Highway Bridges,* Fifteenth Edition and 1993 Interim, Washington, D.C., 1992.
2. Park, R., and Pauley, T., *Reinforced Concrete Structures,* Wiley Interscience, 1975.

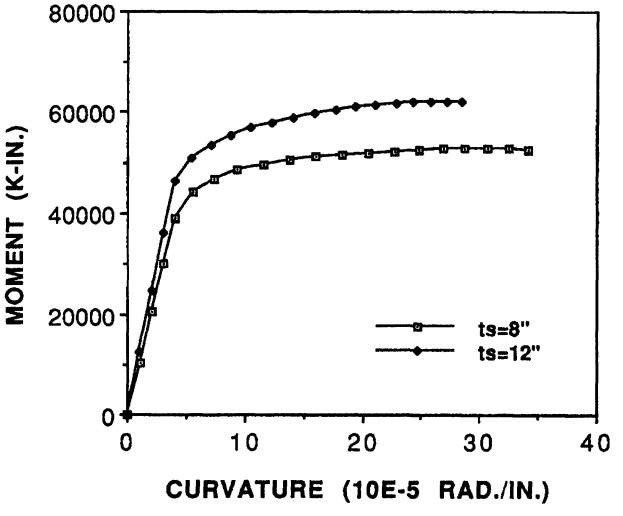

Fig. 13. Effect of concrete slab thickness on M–ϕ curve.

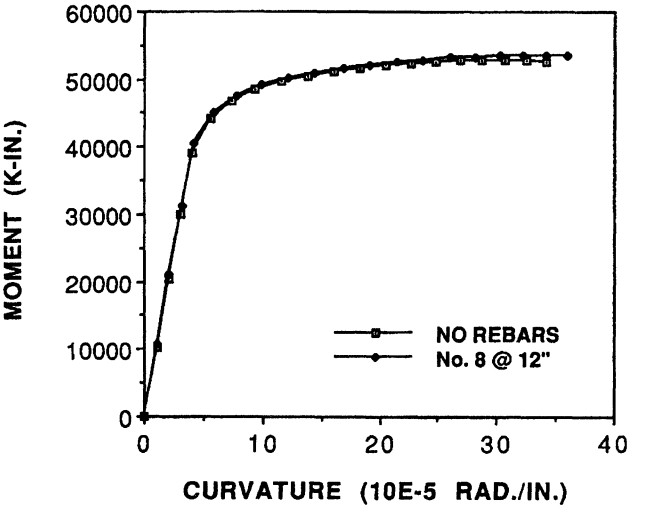

Fig. 15. Effect of concrete slab reinforcement on M–ϕ curve.

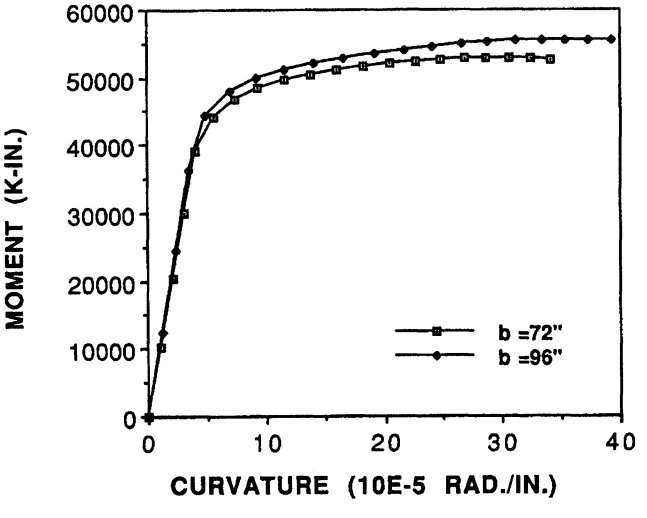

Fig. 14. Effect of concrete slab width on M–ϕ curve.

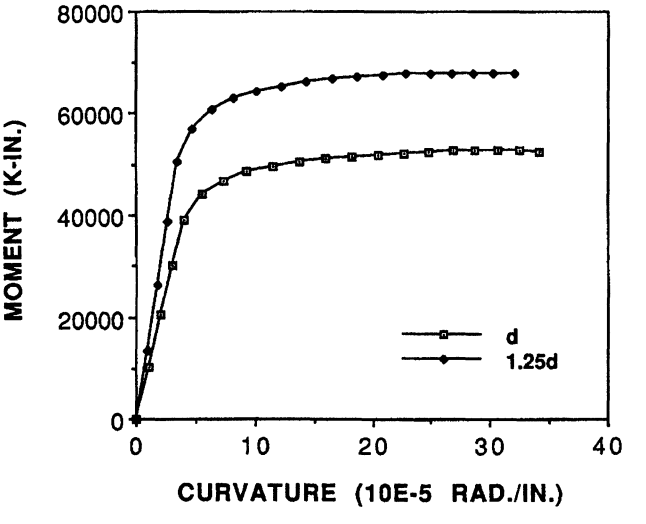

Fig. 16. Effect of steel beam depth on M–ϕ curve.

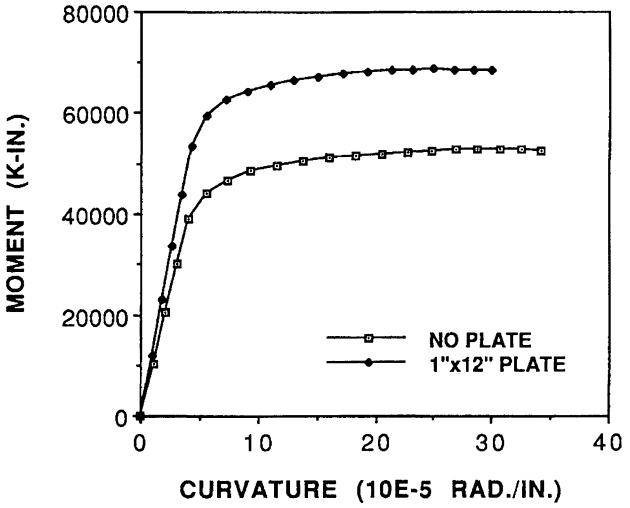

Fig. 17. Effect of cover plate on M–ϕ.

3. Tantawi, H. M., *Ultimate Strength of Highway Girder Bridges,* Ph.D. Thesis, Department of Civil Engineering, University of Michigan, 1986.
4. Kent, D. C., and Park, R., "Flexural Members with Confined Concrete," *Journal of the Structural Division,* ASCE, Vol. 97, No. ST7, July 1971, pp. 1969–1990.
5. Wang, C-K, and Salmon, C. G., *Reinforced Concrete Design,* Fourth Edition, Harper and Row, New York, 1985.
6. Salmon, C. G., and Johnson, E. J., *Steel Structures—Design and Behavior,* Second Edition, Harper and Row, New York, 1980.